Human Molecular Genetics, 2012, Vol. 21, No. 23 ***5078–5090***
doi:10.1093/hmg/dds354
Advance Access published on August 24, 2012

IKAP expression levels modulate disease severity in a mouse model of familial dysautonomia

Paula Dietrich, Shanta Alli, Revathi Shanmugasundaram† and Ioannis Dragatsis*

Department of Physiology, The University of Tennessee, Health Science Center, Memphis, TN 38163, USA

Received May 4, 2012; Revised July 4, 2012; Accepted August 17, 2012

Hereditary sensory and autonomic neuropathies (HSANs) encompass a group of genetically inherited disorders characterized by sensory and autonomic dysfunctions. Familial dysautonomia (FD), also known as HSAN type III, is an autosomal recessive disorder that affects 1/3600 live births in the Ashkenazi Jewish population. The disease is caused by abnormal development and progressive degeneration of the sensory and autonomic nervous systems and is inevitably fatal, with only 50% of patients reaching the age of 40. FD is caused by a mutation in intron 20 of the Ikbkap gene that results in severe reduction in the expression of its encoded protein, inhibitor of kappaB kinase complex-associated protein (IKAP). Although the mutation that causes FD was identified in 2001, so far there is no appropriate animal model that recapitulates the disorder. Here, we report the generation and characterization of the first mouse models for FD that recapitulate the molecular and pathological features of the disease. Important for therapeutic interventions is also our finding that a slight increase in IKAP levels is enough to ameliorate the phenotype and increase the life span. Understanding the mechanisms underlying FD will provide insights for potential new therapeutic interventions not only for FD, but also for other peripheral neuropathies.

INTRODUCTION

Familial dysautonomia (FD), also known as 'Riley-Day syndrome' or 'hereditary sensory and autonomic neuropathy (HSAN) type III', is an autosomal recessive disorder that affects almost exclusively the Ashkenazi Jewish population (1/3600 live births), although non-Jewish cases have also been reported (MIM 223900). This debilitating disorder is characterized by impaired development and progressive degeneration of the sensory and autonomic nervous systems (1–3). Neuronal numbers in the dorsal-root ganglia and the superior cervical sympathetic ganglia (SCG) are reduced already in early childhood and progressively decline with age. Pathological findings include a marked decrease in unmyelinated fibers and significant reduction in the innervation of target tissues (4–7). The criteria for the diagnosis of FD are: absence of fungiform papillae on the tongue, absence of flare after intradermal injection of histamine, decreased or absence of deep-tendon reflexes, absence of overflow emotional tears as well as impaired pain and temperature perception (2,5,6,8–10). Other clinical features include gastrointestinal dysfunction, gastroesophageal reflux, vomiting crises, recurrent pneumonia, seizures, gait abnormalities, kyphoscoliosis, repeated fevers, postural hypotension and hypertension crises. Despite advances in patient care, the disorder is inevitably fatal, with only 50% of patients reaching 40 years of age (3).

Mutations in the Ikbkap gene (mapped to human chromosome 9q31) were shown to cause FD (11,12). In humans, the *Ikbkap* gene covers a 68 kb genomic sequence containing 37 exons and encodes a 150 kDa protein named inhibitor of kappaB kinase complex-associated protein (IKAP). In FD the major haplotype (representing >98% of the FD cases) is associated with a T to C transition in position 6 of the donor splice site of intron 20 of the *Ikbkap* gene (11,12). This mutation results in the generation of an mRNA in which exon 20 (74 bp) is spliced out, along with intron 20, causing a frameshift and producing a putative truncated protein of 79 kDa. However, patients with FD continue to express the wild-type (WT) message in all tissues, with nervous system tissues displaying severely reduced amounts of the WT mRNA (12,13). Interestingly, despite the fact that most FD patients carry the same mutation, the severity of the disease is highly variable, both between and within families (14,15). This observation

*To whom correspondence should be addressed at: Department of Physiology, The University of Tennessee, Health Science Center, 894 Union Avenue, room 502, Nash BLDG, Memphis, TN 38163, USA. Tel: +1 9014483615; Fax: +1 9014487126; Email: idragatsis@uthsc.edu
†Present address: Department of Animal Sciences, The Ohio State University, 1680 Madison Avenue, Wooster, OH 44691 USA.

led to the suggestion that this variability might be a consequence of differences in the extent of exon 20 skipping between individuals, either in specific tissues or at specific stages of development (12). However, the possible correlation between levels of expression and disease severity is still speculative.

IKAP was originally identified and named due to its ability to bind IκB kinases and assemble them into an active kinase complex (16). However, subsequent studies suggested that IKAP might be directly involved in RNA polymerase II transcription elongation. Notably, IKAP shares high homology with the yeast elongator protein 1 (Elp1), co-purifies with the human Elongator complex, directly binds to DNA sequences and regulates the expression of several genes (17–19), indicating that IKAP is the mammalian Elp1 homolog (although Elp1 is a synonym of IKAP, we will use the OMIM and MGI nomenclature, IKAP for the protein and Ikbkap for the gene). On the other hand, IKAP is mainly a cytoplasmic protein (16,19), and several lines of evidence indicate that it also participates in other cellular processes such as cell migration and cytoskeleton organization (20,21), Jun N-terminal kinase (JNK)-mediated stress signaling (22), exocytosis and tRNA modification (23–25). Down-regulation or silencing of IKAP in cellular systems or *in vivo* suggests that IKAP may be involved in multiple biological processes, including cell migration, cell proliferation and differentiation and regulation of apoptosis (19,20,26–29). Despite all these findings, the mechanisms by which decreased IKAP levels result in FD still remain to be elucidated. The generation of a suitable animal model that recapitulates FD molecular and phenotypic features would therefore be invaluable to further understand the complex pathophysiology of the disease, to accelerate the development of alternative therapeutic strategies, and provide more information regarding the processes that regulate normal peripheral nervous system (PNS) development.

In the mouse, the *Ikbkap* gene is located on chromosome 4 in a region that is syntenic to human chromosome 9q31.3. As in humans, the *Ikbkap* gene is also organized in 37 exons (distributed over ∼51 kb of genomic DNA) and encodes a protein of 1332 amino acids with a molecular weight of ∼150 kDa (30,31). The mouse IKAP protein shows a high degree of homology with the human IKAP, with 80% amino acid identity. The consensus donor splice site of intron 20, which is mutated in the major FD haplotype, is conserved in the mouse. However, attempts to generate a mouse model for FD by introducing the FD major haplotype mutation in the mouse genome have so far been unsuccessful. As part of our efforts to understand and model FD, we have previously generated and characterized mice carrying a 3loxP-targeted *Ikbkap* allele (*Ikbkap*^{3loxP}, Mouse Genome Informatics designation: Ikbkap^{tm1Id}) and an exon 20 deletion allele (*Ikbkap*$^{\Delta 20}$, Mouse Genome Informatics designation; Ikbkap$^{tm1.1Id}$). Mice homozygous for the *Ikbkap*$\Delta 20$ allele are identical to null embryos and display growth retardation and severe cardiovascular defects and die early in embryogenesis, and hence do not constitute a mouse model for the disease (32). Here, we report the generation and characterization of two mouse models of FD that recapitulate the phenotypic spectrum of FD. Comparative analyses of these models indicate that a slight increase in the levels of IKAP expression greatly diminishes the severity of the disorder and also leads to a significant increase in life span.

RESULTS

Generation of two FD mouse models

Attempts by our laboratory and others to generate a mouse model for FD either by introducing the FD major haplotype mutation in the mouse *Ikbkap* locus as a knockin or by introducing a humanized FD BAC transgene in the mouse genome have so far been unsuccessful (P. Dietrich, unpublished data; D. Brenner, personal communication; S. Slaugenhaupt, personal communication; G. Ast, personal communication). Since full-length IKAP expression levels are particularly low in nervous system tissues of FD patients, we reasoned that conditional inactivation of the Ikbkap gene specifically in neuronal cells might represent an alternative approach to generate a model for FD.

For the generation of the *Ikbkap* conditional allele, we crossed mice carrying a 3loxP-targeted *Ikbkap* allele (*Ikbkap*$^{3loxP/+}$; 32) with a Cre transgenic line that results in partial recombination events (33). Selected mosaic F1 progeny carrying the desired recombinant alleles were then crossed with WT mice, and resulted in the production of *Ikbkap*$^{flox/+}$ mice Fig. 1A), which are normal and fertile.

Intercrosses between *Ikbkap*$^{flox/+}$ mice revealed that *Ikbkap*$^{flox/flox}$ mice were born at Mendelian ratio, but were smaller than control littermates and a significant fraction of these mice (∼95%) died perinatally. These observations led us to examine whether the presence of the loxP sites might have affected the expression of the targeted allele. Western analyses on protein extracts from brains of WT and *Ikbkap*$^{flox/+}$, *Ikbkap*$^{flox/flox}$ littermates, as well as from *Ikbkap*$^{\Delta 20/+}$ (mice heterozygous for an Ikbkap exon 20 deletion allele; 32) age-matched mice (Fig. 1B) indicated that the IKAP protein level in *Ikbkap*$^{flox/+}$ brains was ∼50% the levels of WT controls, and was similar to that of *Ikbkap*$^{\Delta 20/+}$ brains, suggesting that the insertion of the loxP sites in intronic regions of the Ikbkap gene interfered with the normal expression of the targeted allele and resulted in severely reduced levels of the expression of the full-length IKAP protein. Quantitative analyses indicated that IKAP expression in *Ikbkap*$^{flox/flox}$ brains is ∼10% that of WT mice (Fig. 1D).

Since FD is caused by severe reduction in the expression of the full-length IKAP protein (11–13), we examined whether *Ikbkap*$^{flox/flox}$ or compound heterozygous *Ikbkap*$^{\Delta 20/flox}$ mice represent a model for FD. For this purpose, we generated and analyzed in parallel *Ikbkap*$^{flox/flox}$ and *Ikbkap*$^{\Delta 20/flox}$ mice derived from *Ikbkap*$^{flox/+}$ and *Ikbkap*$^{\Delta 20/+}$ crosses. At birth, *Ikbkap*$^{\Delta 20/flox}$ mice appeared grossly normal but were significantly smaller than their WT or heterozygous littermates. Similar to the severely affected FD patients, the majority of the *Ikbkap*$^{\Delta 20/flox}$ pups were born with ∼70% the weight and size of their littermates, and without any intervention all of them died during the first postnatal days from starvation as they failed to suck milk/or swallow efficiently—newborn *Ikbkap*$^{\Delta 20/flox}$-mutant pups could easily be identified at birth as those lacking milk in their stomachs. Western analyses confirmed that, as expected, *Ikbkap*$^{\Delta 20/flox}$ expressed about half the

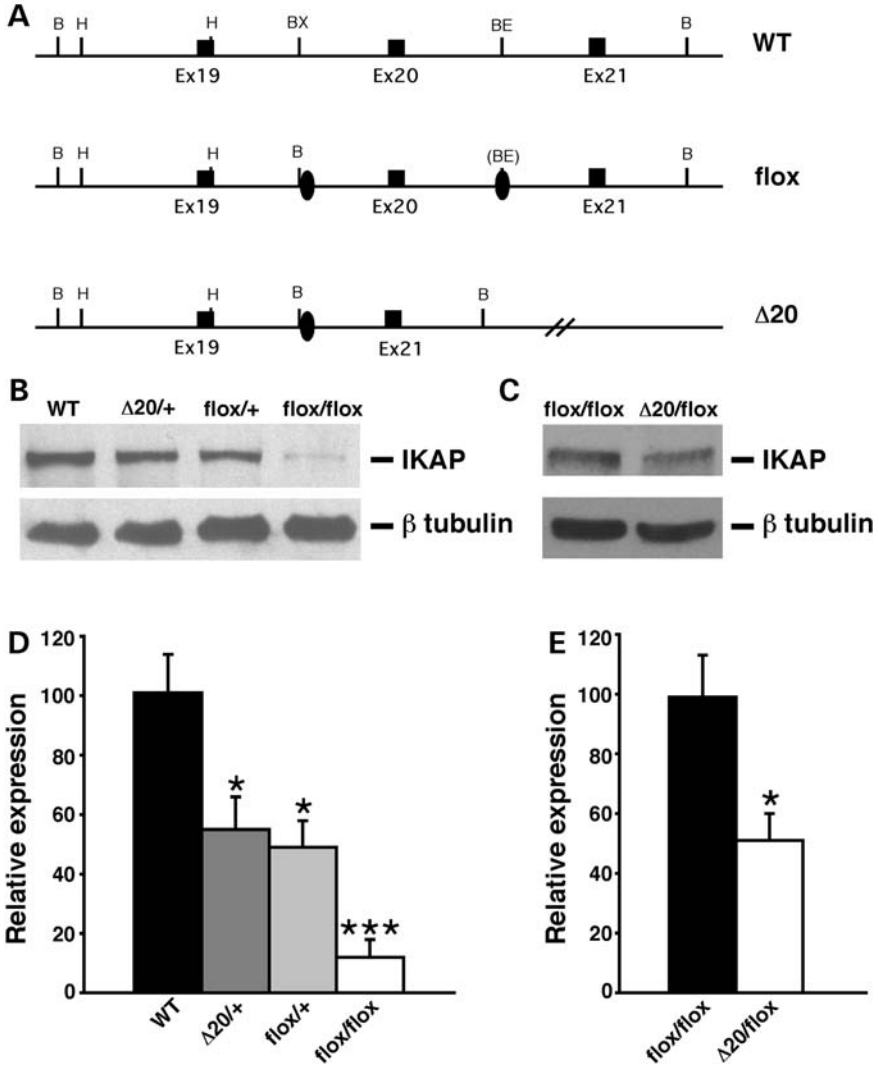

Figure 1. Generation and molecular characterization of FD mouse models. (**A**) Schematic representation of the wild-type allele (WT), Ikbkapflox allele (flox) and Ikbkap allele lacking exon 20 (Δ20). Exons are represented by black rectangles, and the loxP sites by black ovals. Restriction sites shown on the schematic are: Bam HI (B), HindIII (H), BstXI (BX) and BstEII (BE). (**B**) Western analyses of total protein lysates from the forebrain of 11-month-old WT, *Ikbkap*$^{\Delta 20/+}$, *Ikbkap*$^{flox/+}$ and *Ikbkap*$^{flox/flox}$ mice. The upper panel shows the detection of IKAP with the polyclonal anti-IKAP antibody (AnaSpec), and the lower panel shows anti-β-tubulin staining for loading control. Note that the IKAP protein level is severely reduced in *Ikbkap*$^{flox/flox}$ brain. (**C**) Western analyses of total protein lysates from the whole brain of E16.5 *Ikbkap*$^{flox/flox}$ and *Ikbkap*$^{\Delta 20/flox}$ embryos. The upper panel shows the detection of IKAP with the polyclonal anti-IKAP antibody (AnaSpec), and the lower panel shows anti-β-tubulin staining for loading control. Note that in the *Ikbkap*$^{\Delta 20/flox}$ brain IKAP protein expression is reduced compared with the *Ikbkap*$^{flox/flox}$ brain. (**D** and **E**) Quantitative analyses of IKAP expression levels in mouse brains of different genotypes. (**D**) IKAP expression levels were normalized over tubulin levels and are expressed as percentage of WT. (**E**) IKAP expression levels were normalized over tubulin levels and are expressed as percentages of *Ikbkap*$^{flox/flox}$. Data are represented as mean ± SD; $n = 3$ experiments. $^{*}P < 0.05$, $^{***}P < 0.001$.

levels of full-length IKAP compared with *Ikbkap*$^{flox/flox}$ mutants (Fig. 1C and E), equivalent to 5% the levels of WT mice.

These initial observations suggested that both *Ikbkap*$^{\Delta 20/flox}$ and *Ikbkap*$^{flox/flox}$ might constitute two complementary models for FD, with symptoms being severe in *Ikbkap*$^{\Delta 20/flox}$ mice and milder in *Ikbkap* $^{flox/flox}$ mice. To further characterize these mice as possible mouse models for FD, and to evaluate to what extent the phenotypic expression of FD is ameliorated due to the slight increase in IKAP in *Ikbkap*$^{flox/flox}$ mice, we assessed several FD phenotypic features in these two mutant lines in parallel.

Embryonic growth and early postnatal characteristics

FD neonates weigh significantly less (75–85%) than their normal siblings, due to intrauterine growth retardation (34). At birth, both *Ikbkap*$^{\Delta 20/flox}$ and *Ikbkap*$^{flox/flox}$ mice were consistently smaller than their control littermates, indicating that reduced IKAP expression significantly affected their embryonic growth. Analyses of litters at different stages during embryogenesis showed that, starting at mid-gestation, both *Ikbkap*$^{\Delta 20/flox}$ and *Ikbkap*$^{flox/flox}$ embryos had a significantly reduced growth rate compared with their control littermates (Table 1). In addition, we found that placenta growth was

Table 1. Embryonic and postnatal growth

	E14.5	E16.5	E18.5	P15	P21
WT	204.2 ± 13.8 ($n = 7$)	492.1 ± 14.6 ($n = 10$)	1207.7 ± 26.8 ($n = 20$)	9.05 ± 0.20 ($n = 9$)	12.59 ± 0.40 ($n = 10$)
Ikbkap$^{flox/flox}$	179.3 ± 1.7 ($n = 3$)	386.0 ± 5.5** ($n = 5$)	1017.4 ± 39.6*** ($n = 10$)	5.85 ± 0.08*** ($n = 6$)	8.33 ± 0.63* ($n = 4$)
Ikbkap$^{\Delta 20/flox}$	146.5 ± 19.9* ($n = 4$)	312.5 ± 7.0*** ($n = 4$)	795.5 ± 24.1*** ($n = 12$)	4.00 ± 0.26*** ($n = 3$)	5.10 ± 0.15*** ($n = 4$)

Values represent mg for embryonic days and g for postnatal days.
Ikbkap$^{\Delta 20/flox}$ weights are statistically different from *Ikbkap*$^{flox/flox}$ weights ($P < 0.01$) for all timepoints except E14.5.
Data presented are expressed as mean ± SEM. Student's *t*-test was employed with $^{*}P < 0.05$, $^{**}P < 0.01$, $^{***}P < 0.001$.

also significantly affected, averaging 55% the size of WT placentas for *Ikbkap*$^{\Delta 20/flox}$ embryos and 75% for *Ikbkap*$^{flox/flox}$ embryos from mid-gestation onwards. Histological examination of *Ikbkap*$^{\Delta 20/flox}$ placentas at late gestation revealed that the spongiotrophoblast layer was poorly developed, whereas the labyrinthine zone appeared normal (Supplementary Material, Fig. S1). Although placental development has not been investigated in FD patients, this observation suggests that impaired placental development may contribute to embryonic growth retardation in FD.

Since the average mouse litter size is 8–12 pups, and female mice have the tendency to concentrate on pups that have the highest chances for survival, trimming the litters at birth allowed for reduction in competition between siblings, and the survival of ~5% of *Ikbkap*$^{\Delta 20/flox}$ mutants. At postnatal days 18–21 (P18-P21), *Ikbkap*$^{\Delta 20/flox}$ mice were ~32% the weight of their WT littermates (Fig. 2A), they displayed poor locomotor coordination, unsteady gait and postural instability, and appeared to be hypersensitive to handling. Owing to the low body weight and poor health, most of the mutants had to be sacrificed between P18 and P21. Autopsy of the mutant pups revealed that they had almost no fat content and had bubbles of air in their intestines, suggestive of gastrointestinal dysfunction (Supplementary Material, Fig. S2). In contrast, trimming of the litters at birth allowed 20% of *Ikbkap*$^{flox/flox}$ mice to survive postnatally. Although the postnatal growth of *Ikbkap*$^{flox/flox}$ mice was also compromised, at P21 *Ikbkap*$^{flox/flox}$ mice were 70–80% the weight of their control littermates, a significant improvement compared with *Ikbkap*$^{\Delta 20/flox}$ mice of the same age.

One of the hallmarks of FD is severely reduced numbers of fungiform papillae on the tongue. This feature of FD patients is observed already in infants and varies from severely reduced numbers to complete lack of taste-bud papillae on the tip of the tongue, giving it a smooth appearance (8,35). To assess whether there was a reduction in the number of fungiform papillae on the tongue of *Ikbkap*$^{\Delta 20/flox}$ and *Ikbkap*$^{flox/flox}$ mice, we analyzed mutant and control tongues at P18. Methylene blue staining revealed a significant reduction in the total number of fungiform papillae in mutant mice compared with WT littermates. While the average number of fungiform papillae on a WT tongue was 86 ± 8 ($n = 4$), the total number averaged 47 ± 8 in *Ikbkap*$^{\Delta 20/flox}$ mice ($n = 4$) and 60 ± 7 in *Ikbkap*$^{flox/flox}$ mice ($n = 5$). Histological examination revealed that although fungiform papillae of mutant tongues possessed a well-developed taste bud, their distribution—especially in the anterior portion of the tongue—was more sparse, and a significant fraction of them did not appear healthy and were smaller than those of control tongues (Fig. 2B and C).

Phenotypic and behavioral characteristics in adulthood

With the use of experienced breeders, trimming the litters at birth and keeping the surviving FD mutants and control littermates with their parents for one extra month after they had reached weaning age, six *Ikbkap*$^{\Delta 20/flox}$ and twenty-eight *Ikbkap*$^{flox/flox}$ mice survived till adulthood (10 months and older). In both cases, the mutant mice displayed excessive grooming, self-inflicted wounds from frequent scratching and several neurological symptoms including ataxic gait, hindlimb clasping on tail suspension (Supplementary Material, Fig. S3) and handling-induced seizures. Also, similar to post-adolescent and adult patients with FD who are short in stature (5′2″ for males and 4′10″ for females, i.e. ~85% the height of normal siblings) and very thin (2,36), *Ikbkap*$^{\Delta 20/flox}$ and *Ikbkap*$^{flox/flox}$ mice (>11 months of age) were short in length (~85–90% the length of their control littermates), displayed low body weight (Fig. 2D) and very little fat content.

In addition, 100% of *Ikbkap*$^{\Delta 20/flox}$ mice analyzed (6 out of 6) and ~75% of *Ikbkap*$^{flox/flox}$ mice (20 out of 28) also developed skeletal abnormalities, mostly kyphosis or kyphoscoliosis (Fig. 2E–H) that worsened over time. Interestingly, these mice also exhibited an abnormal postural behavior (sitting-up), which was not observed in their control littermates (Fig. 2I). Although the reason for this behavior is currently not known, we speculate that it might represent an effort to compensate for the kyphoscoliosis.

With increasing age, a large number of the mutant mice also exhibited additional phenotypes related to dysautonomia. Blepharoptosis (drooping of the upper eyelid) and conjunctivitis (an early symptom of dry eye) were observed in four out of six (66.7%) of *Ikbkap*$^{\Delta 20/flox}$ mice and ~40% of *Ikbkap*$^{flox/flox}$ mice. Urine retention/neurogenic bladder (bladder distension, Fig. 2F) and/or hydronephrosis was observed in 2 out of 3 *Ikbkap*$^{\Delta 20/flox}$ adult males and in 5 out of 17 *Ikbkap*$^{flox/flox}$ males starting at 11 months of age, with partial or complete destruction of one of the kidneys observed in three of them (Supplementary Material, Fig. S4). Chronic kidney disease (CKD) is an increasingly common complication of FD, with half of the patients reaching stage 3 CKD by the age of 25 (37). Although hydronephrosis has been observed in ~10% of young FD patients, its cause is currently unknown (38). Our results suggest that neurogenic bladder might be the

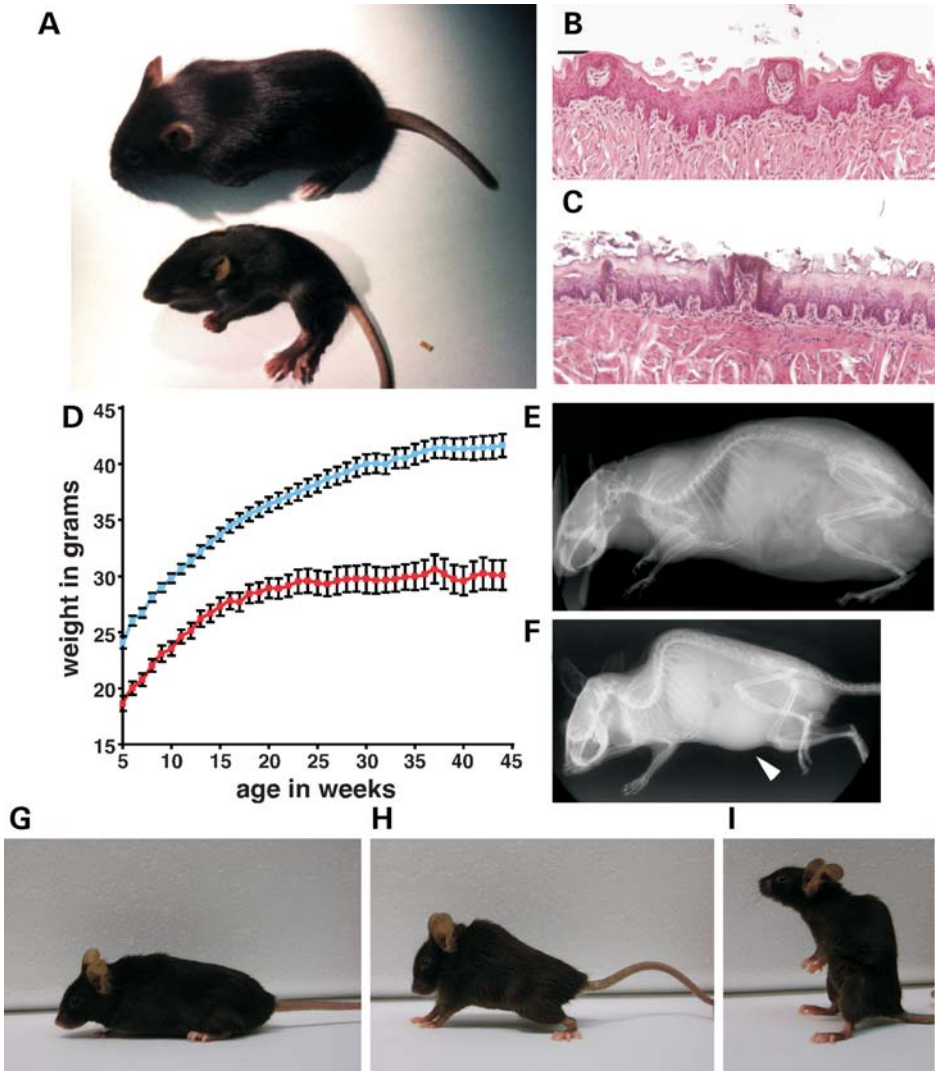

Figure 2. Postnatal characteristics of *Ikbkap*$^{\Delta 20/flox}$ and *Ikbkap*$^{flox/flox}$ mice. (**A**) Appearance of *Ikbkap*$^{\Delta 20/flox}$ mice at P18. WT (top) and *Ikbkap*$^{\Delta 20/flox}$ (bottom) littermates were photographed side by side. Note that the mutant *Ikbkap*$^{\Delta 20/flox}$ mouse is significantly smaller than its WT littermate and exhibits abnormal posture and puffy feet. (**B** and **C**) Representative histological examinations of tongue fungiform papillae. Tongues of P18 WT (**B**) and *Ikbkap*$^{\Delta 20/flox}$ (**C**) littermates were processed for paraffin embedding, and coronal sections of the anterior part of the tongue were stained with H&E. Note that the three fungiform papillae of the WT littermates appear normal (**B**), whereas in the mutant the fungiform papilla shown is degenerating (**C**). (**D**) Postnatal growth curves of control (blue, $n = 37$) and *Ikbkap*$^{flox/flox}$ (red, $n = 14$) male mice. Similar results were found for female mice. Data are represented as mean $\pm$ SEM. (**E** and **F**) MicroCT scans of 11-month-old WT (**E**) and *Ikbkap*$^{\Delta 20/flox}$ (**F**) littermate male mice. Note that the mutant is significantly smaller than the control and displays a severe curvature of the spine (kyphosis). In this scan, a significant enlargement of the bladder is also observed in the mutant (arrowhead). (**G**–**I**) 16-month-old WT (**G**) and *Ikbkap*$^{flox/flox}$ (**H** and **I**) female littermates. Note the spinal curvature of the mutant (**H**) and the sitting-up posture (**I**) that it assumes frequently.

primary cause of reflux/hydronephrosis, and a possible contributing factor to renal failure in FD.

Unfortunately, since mice do not sweat and do not have a gagging reflex, the typical symptoms of dysautonomic crisis of FD patients which are elicited by stress/emotional arousal could not be assessed in these mouse models. However, *Ikbkap*$^{\Delta 20/flox}$ and *Ikbkap*$^{flox/flox}$ mice frequently exhibited abnormally exaggerated reactions to stressful situations. For instance, excessive handling or loud startling noise induced seizures, and the discomfort caused by temperature perception tests led to an exaggerated nocifensive response (jumping multiple times beyond 20 cm of height), which persisted after the noxious stimulus has ceased. In contrast, control age-matched littermates did not experience seizures, and exhibited only a mild nocifensive reaction to noxious stimuli that stopped immediately when conditions were back to normal.

Life span and overall health of the mutant mice were also compromised, but less so for *Ikbkap*$^{flox/flox}$ mice. Of the six surviving adult *Ikbkap*$^{\Delta 20/flox}$ mice, four had to be sacrificed prior to 18 months of age, and only two reached 22 months of age but with serious health problems, including prominent ataxic gait, reduced locomotion activity, pronounced kyphosis and severe weight loss. In contrast, 15 of 28 (54%) *Ikbkap*$^{flox/flox}$ mice survived past 18 months

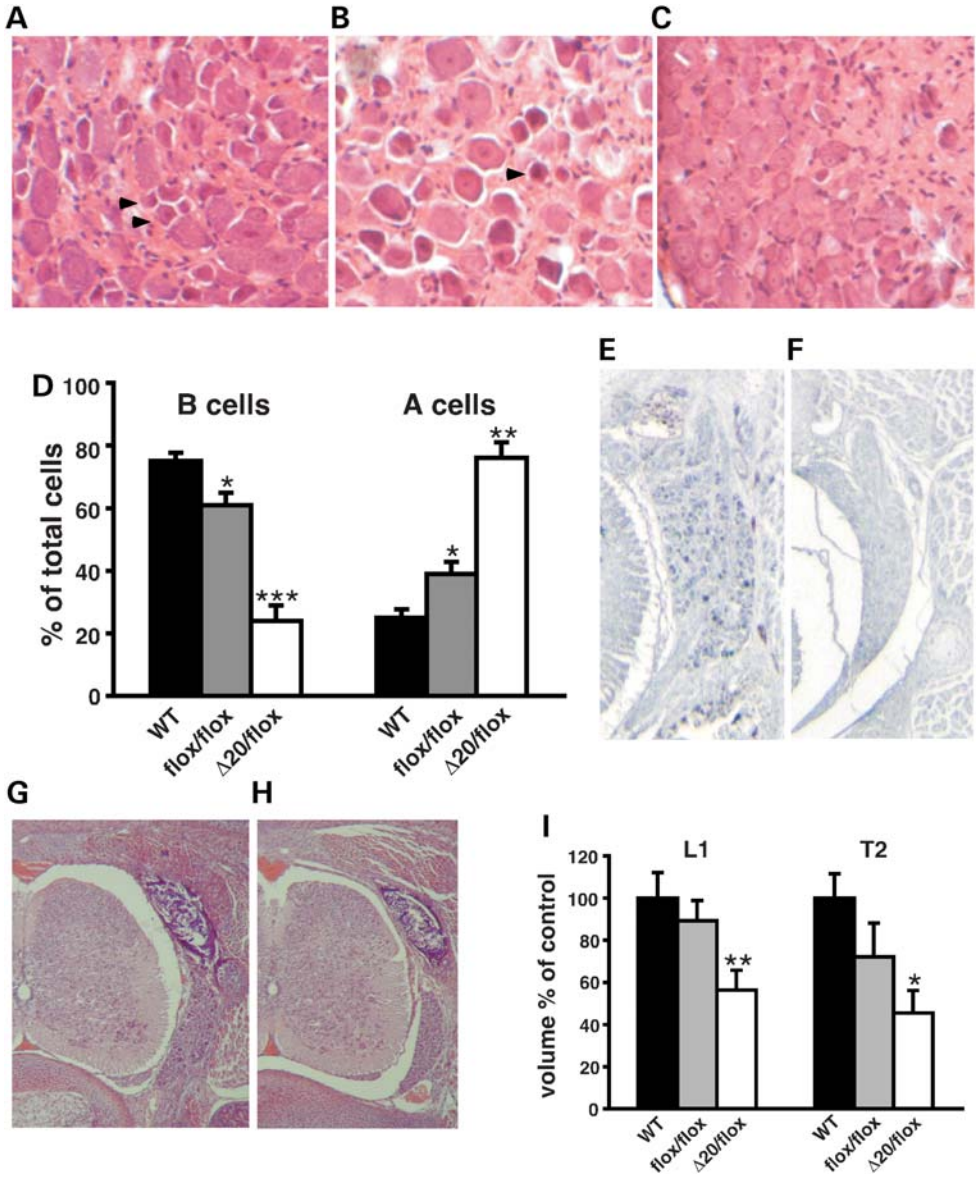

Figure 3. Sensory ganglia deficits in FD mouse models. (**A**–**C**) Representative H&E-stained cross sections through thoracic DRGs of 18-month-old WT (**A**), *Ikbkap*$^{flox/flox}$ (**B**) and *Ikbkap*$^{\Delta 20/flox}$ (**C**) mice. Note that the DRGs of WT and *Ikbkap*$^{flox/flox}$ mice contain numerous small dark neurons (arrowheads), which are virtually absent in *Ikbkap*$^{\Delta 20/flox}$ DRGs. (**D**) Quantification of small dark (type B) and large light (type A) neuronal profiles in 18-month-old WT, *Ikbkap*$^{flox/flox}$ and *Ikbkap*$^{\Delta 20/flox}$ DRGs ($n = 3$). Percentages of type A and type B neuronal cells over the total number of cells are displayed ($n = 3$). (**E** and **F**) Transverse paraffin sections of E18.5 WT (**E**) and *Ikbkap*$^{\Delta 20/flox}$ (**F**) embryos were immunostained with anti-CGRP antibody. Note the large number of CGRP-positive neuronal cells in WT DRG in contrast to their near absence in *Ikbkap*$^{\Delta 20/flox}$ mutant DRG. (**G** and **H**) H&E-stained transverse sections of WT (**G**) and *Ikbkap*$^{\Delta 20/flox}$ (**H**) E18.5 embryos show that the DRG is significantly reduced in the size in the mutants already at this stage. (**I**) Volumes of lumbar L1 DRG (L1) and thoracic T2 (T2) of E18.5 WT ($n = 4$), *Ikbkap*$^{flox/flox}$ ($n = 3$) and *Ikbkap*$^{\Delta 20/flox}$ embryos ($n = 3$). Data are expressed as mean ± SD. $^{*}P < 0.05$, $^{**}P < 0.01$, $^{***}P < 0.001$.

of age and, of these, 7 lived up to 22–24 months of age with minor health problems. These observations indicate that although *Ikbkap*$^{flox/flox}$ mice also develop FD phenotypic features, the slight increase in IKAP expression has a significant impact on their overall health and longevity.

Sensory ganglia deficits

In FD, quantitative studies on dorsal root ganglia (DRGs) have shown that in very young patients the DRG neuronal numbers are already 20% of controls (39). Consistent with these observations, temperature and pain perception are already altered in infancy (14). Furthermore, worsening of nociception over time also suggests that the number of nociceptive neurons in DRGs progressively decline with age (14).

Based on their morphology and cytochemical characteristics, sensory neurons of the DRG in adult rodents are classified into two major classes, large light type A cells (25–30% of total neurons) and small dark B cells, representing 70–75% of total neurons (40–42). Strikingly, at 18 months of age the relative proportion of small dark B cells in lumbar DRGs was extremely reduced in *Ikbkap*$^{\Delta 20/flox}$ mice compared with

controls, whereas *Ikbkap*$^{flox/flox}$ exhibited a smaller but significant decrease (Fig. 3A–D). The reduction in type B cells is consistent with both the decrease in temperature and pain perception and the reduced number of unmyelinated fibers observed in FD patients, since most unmyelinated fibers conducting pain and thermal perception originate from type B cells (43–45). Consistent with these observations, temperature perception was also impaired in our FD mouse models (Supplementary Material, Fig. S5).

To assess whether the reduction in DRG nociceptive type B cells observed in adult *Ikbkap*$^{\Delta 20/flox}$ mice is due to abnormal embryonic development of sensory ganglia or to progressive postnatal neurodegeneration, serial transverse and coronal sections of embryonic day 18.5 (E18.5) WT and *Ikbkap*$^{\Delta 20/flox}$ and *Ikbkap*$^{flox/flox}$ embryos spanning thoracic and lumbar DRGs were analyzed. As shown in Figure 3G–I, the volumes of lumbar and thoracic DRGs were already significantly reduced in *Ikbkap*$^{\Delta 20/flox}$ mutant embryos compared with their WT littermates, whereas they were only marginally reduced in *Ikbkap*$^{flox/flox}$ embryos. Notably, nociceptive neurons [trkA/calcitonin gene-related peptide (CGRP) positive neurons] were already extremely reduced in numbers in *Ikbkap*$^{\Delta 20/flox}$ mutants at E18.5 (Fig. 3E and F). Our results corroborate the hypothesis that embryonic development of sensory ganglia is majorly compromised in patients with severe FD, and suggest that the postnatal loss of nociceptive neurons is a slow process, as indicated by their relative preservation in 18-month-old *Ikbkap*$^{flox/flox}$ mice.

Sympathetic ganglia deficits

Although the quantification of superior SCG neuronal density and numbers in FD has been so far restricted to the postnatal period, the reduction in neuronal density and neuronal numbers in SCG observed in young FD patients (4,46,47) is generally attributed to abnormal embryonic development, and it is thought to involve either abnormal differentiation or impaired neural crest cell migration (3,19,26). At E18.5, immunohistochemistry for tyrosine hydroxylase (TH) demonstrated correct localization and normal differentiation of sympathetic neurons in SCG, stellate ganglia (SG) and celiac ganglia in both *Ikbkap*$^{flox/flox}$ and *Ikbkap*$^{\Delta 20/flox}$ embryos, suggesting that neither neural crest cell migration nor neuronal differentiation was affected (Supplementary Material, Fig. S6). Histological examination of serial transverse and coronal sections of E18.5 WT, *Ikbkap*$^{flox/flox}$ and *Ikbkap*$^{\Delta 20/flox}$ embryos nevertheless revealed that at late gestation there was indeed already a significant reduction in the volume of SCG and SG in mutant embryos (in particular in *Ikbkap*$^{\Delta 20/flox}$ embryos) compared with WT littermates (Fig. 4A–D). However, contrary to what is observed in young FD patients, neuronal density was not decreased in any of the two FD mouse models at late gestation, and neuronal numbers were not as dramatically reduced as in FD patients (Fig. 4E), suggesting that significant neuronal loss must be occurring postnatally.

To determine the extent of postnatal neuronal loss, we analyzed SCGs of *Ikbkap*$^{flox/flox}$ and controls at weaning age (P21) and at 10 months of age, around the time when additional phenotypes related to dysautonomia were clearly visible (see above). At P21, although the total volume of SCG was ~80% the volume of controls, neuronal cells were less densely packed. By 10 months of age, both volume and neuronal density of SCGs were significantly reduced in *Ikbkap*$^{flox/flox}$ mice compared with controls, with the volume of SCG being as low as 30% of control littermates (Fig. 4F and G). Neuronal counts at P21 and 10 months of age revealed a striking progressive decrease in neuronal numbers in the postnatal period in *Ikbkap*$^{flox/flox}$ mice compared with controls (Fig. 4H). Our results suggest that although abnormal embryonic development of SCG does occur in FD, it is mostly postnatal neuronal loss that accounts for the severe reduction in overall neuronal numbers and neuronal density in SCG observed in young as well as adult FD patients (4,46).

Other histopathological findings

Optic atrophy is an increasingly prevalent characteristic of FD patients as they age and appears to worsen over time (48,49). More recently, it has been shown that patients with FD have a specific type of optic neuropathy with predominant loss of papillomacular nerve fibers (50). Since reduction in the papillomacular bundle is due to loss of parvocellular-projecting retinal ganglion cells (RGCs), we performed histological analyses on the retina and optic nerve of 22-month-old *Ikbkap*$^{\Delta 20/flox}$ ($n = 2$), *Ikbkap*$^{flox/flox}$ ($n = 3$) and control ($n = 5$) mice. We found that in both mouse FD models there was a significant decrease in the convergence of RGCs to the optic nerve in both mouse models, but significantly more pronounced in *Ikbkap*$^{\Delta 20/flox}$ mice (Supplementary Material, Fig. S7).

Recent findings suggest that the hypotonic muscle tone in FD infants, the absence of deep tendon reflexes characteristic of FD patients, as well as the progressive ataxic gait might be due to either agenesis of muscle spindles or loss of muscle spindle sensory afferents (51). Since *Ikbkap*$^{\Delta 20/flox}$ and *Ikbkap*$^{flox/flox}$ mice also exhibit low muscle tone early postnatally and an ataxic gait that worsens over time (see above), we sought to determine whether loss of muscle spindles could be the underlying mechanism. Although there are no histopathological analyses of skeletal muscle from FD patients for comparison, our results indicate that muscle spindles develop normally in *Ikbkap*$^{flox/flox}$ mice ($n = 3$), but exhibit significantly reduced primary sensory afferent innervation (Supplementary Material, Fig. S8). These results suggest that impaired muscle spindle function in FD patients might be due to loss of primary sensory afferent innervation.

DISCUSSION

Attempts by our laboratory and others to generate a mouse model for FD by introducing the FD major haplotype mutation in the mouse Ikbkap locus have so far been unsuccessful. Although the reasons for this failure are still not clear, it has been suggested that the size and/or sequence of the introns surrounding the mutation site might represent a technical impediment, or that differences between the mouse and human splicing machineries might have undermined the success of this approach. Using an alternative approach, we have generated the first animal models that recapitulate the major FD

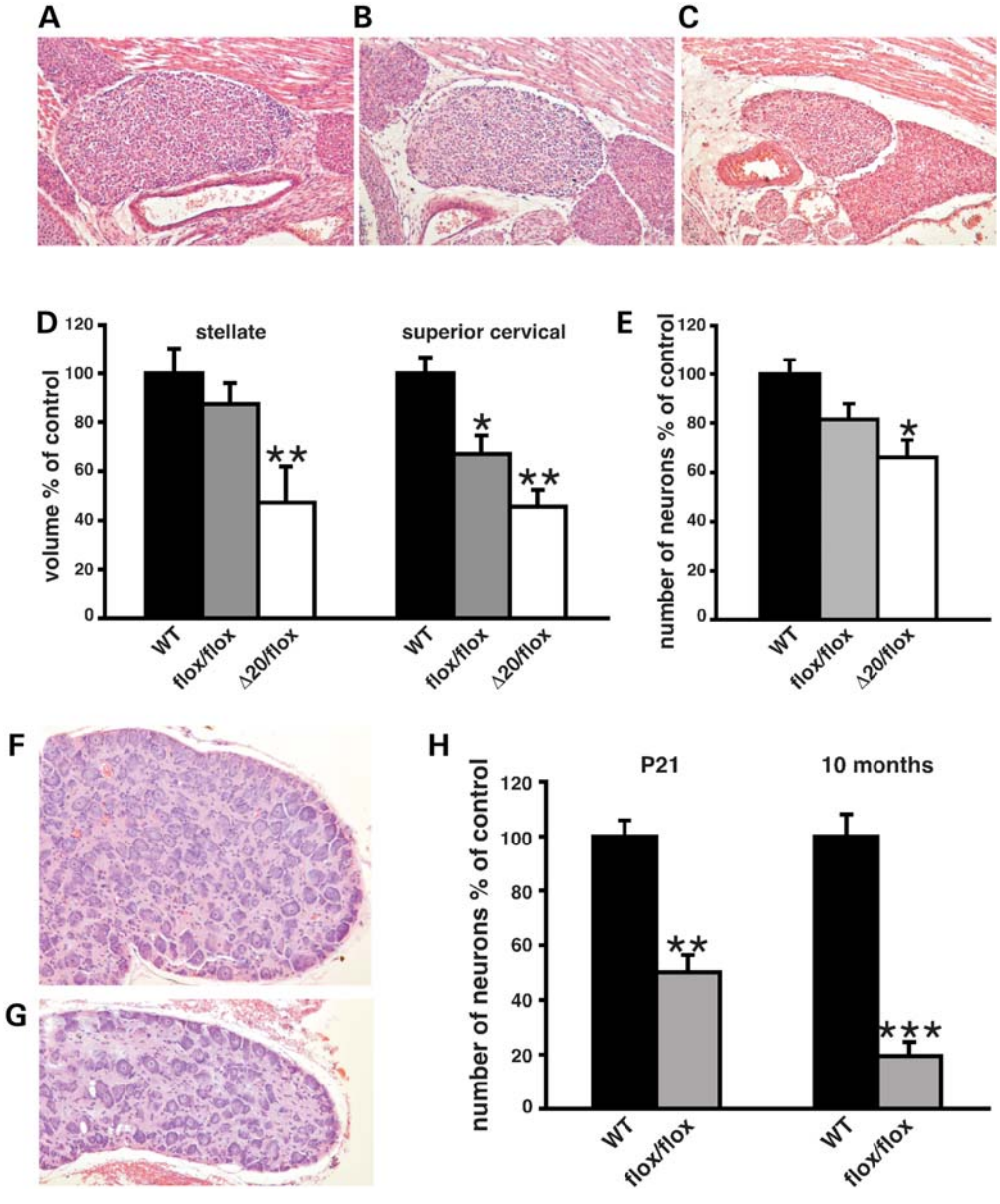

Figure 4. Autonomic deficits in FD mouse models. (**A**–**C**) Representative coronal H&E-stained sections of SCGs of E18.5 WT (**A**), *Ikbkap*$^{flox/flox}$ (**B**) and *Ikbkap*$^{\Delta 20/flox}$ (**C**) at their largest dimensions. (**D**) Volumes of E18.5 stellate and superior cervical sympathetic ganglia of WT, *Ikbkap*$^{flox/flox}$ and *Ikbkap*$^{\Delta 20/flox}$ embryos, displayed as the percentage of controls ($n = 3–5$). (**E**) Neuronal counts of E18.5 SCGs of WT, *Ikbkap*$^{flox/flox}$ and *Ikbkap*$^{\Delta 20/flox}$ embryos are displayed as percentages of controls ($n = 3$). (**F** and **G**) H&E-stained representative cross sections through SCGs of 10-month-old WT (**F**) and *Ikbkap*$^{flox/flox}$ (**G**) mice. Note the smaller size of the mutant SCG as well as the sparse distribution of neurons. (**H**) Neuronal counts of SCGs from P21 and 10-month-old WT and *Ikbkap*$^{flox/flox}$ mice are displayed as percentages of controls. Note that there is a significant decline in neuronal numbers from P21 to 10 months of age in *Ikbkap*$^{flox/flox}$ SCGs relative to controls ($n = 3$). Data are expressed as mean ± SD. $^{*}P < 0.05$, $^{**}P < 0.01$, $^{***}P < 0.001$.

phenotypic and neuropathological features (Table 2), including intrauterine growth retardation, increased perinatal lethality, failure to thrive, reduced number of fungiform papillae on the tongue, gastrointestinal dysfunction, ataxia, skeletal abnormalities, optic neuropathy, seizures and impaired development and maintenance of sensory and autonomic systems. Unfortunately, since mice do not sweat and do not have gagging reflex, the typical symptoms of dysautonomic crisis of FD patients could not be assessed in our FD mouse models. However, similar to FD patients, *Ikbkap*$^{\Delta 20/flox}$ and *Ikbkap*$^{flox/flox}$ mice frequently exhibited abnormally exaggerated reactions to stressful situations such as excessive handling, loud startling noise and noxious stimuli.

Although invaluable cellular systems have been generated in the last few years to model and study FD (19,26,29), FD is a complex disorder and its pleiotropic manifestations can only be fully investigated in the context of a complex organism as the mouse. It is important to note that the cellular systems have been proved successful for testing a plethora of different treatments aimed at restoring splicing with supplements such

Table 2. Ikbkap$^{\Delta 20/flox}$ and Ikbkap$^{flox/flox}$ mouse models reproduce features of FD

	FD patients	Ikbkap$^{\Delta 20/flox}$	Ikbkap$^{flox/flox}$
Reduced expression of full-length IKAP protein	5–20% of controls in CNS	5% of controls in CNS tissues	10% of controls in CNS tissues
Intrauterine growth retardation	+	+	+
Low birth weight	80% of controls	70% of controls	85% of controls
Poor suck, uncoordinated swallow at birth	+	+	+
Poor weight gain	+	+	+
Short stature	+	+	+
Reduced life-span	+	+	+
Dysautonomic crisis	+	N/A	N/A
Seizure susceptibility	+	+	+
Gastrointestinal dysfunction	+	+	+
Absence of overflow emotional tears	+	N/A	N/A
Optic neuropathy	+	+	+
Tongue: Reduced numbers of fungiform papillae	Smooth tongue	45% reduction	30% reduction
Decreased deep tendon reflexes	+	N/D	N/D
Muscle spindle abnormalities	Impaired function	N/D	Reduced sensory innervation
Absent axon flare following intradermal histamine injection	+	N/D	N/D
Poor coordination/balance	+	+	+
Spinal abnormalities	+	+	+
Hydronephrosis	+	+	+
Decreased temperature perception	+	+	+
Decreased volume of DRGs	+	45% of controls at birth	70% of controls at birth
Decreased neuronal numbers in DRGs in adults	10–20% of controls	75% reduction in nociceptive neurons	20% reduction in nociceptive neurons
Decreased volume of sympathetic ganglia at birth	N/D	45% of controls at birth	70% of controls at birth
Decreased volume of SCGs in adults	30% of controls	N/D	30% of controls
Decreased neuronal numbers in SCGs in adults	10% of controls	N/D	20% of controls

+, present; N/A, not applicable; N/D, not determined.

as kinetin (52,53), something that cannot be tested in our mouse models. Our mice, however, are the only *in vivo* models of FD and not only are useful for the elucidation of the pathophysiology of the disease, but are also invaluable for testing the efficacy of current and future therapies that aim at increasing IKAP protein levels through transcriptional activation, such as tocotrienols and phosphatidylserine (54–57).

Our finding that *Ikbkap*$^{\Delta 20/flox}$ mice display a severe reduction in nociceptive (trkA/CGRP positive) neuronal numbers at late gestation is consistent with the severe impairment in pain and temperature perception observed in some FD patients in infancy (1). DRG volumes and total neuronal numbers are also decreased in *Ikbkap*$^{\Delta 20/flox}$ embryos at E18.5 (Fig. 3), suggesting that decreased cell proliferation or increased cell death occurs at earlier stages. Consistent with this hypothesis, silencing of IKAP with shRNA has been shown to result in increased premature neuronal cell death in chick DRGs (58). In marked contrast with what is observed in *Ikbkap*$^{\Delta 20/flox}$ mice, nociceptive neurons appear to be less affected in *Ikbkap*$^{flox/flox}$ mice not only throughout gestation, but also postnatally. These observations indicate that a slight increase in IKAP expression (up to 10% of WT levels) is sufficient to rescue to a great extent DRG neuronal deficits during embryogenesis. In addition, the relative preservation of nociceptive neurons in these mice even in adulthood (Fig. 3) suggests that postnatal degeneration of sensory neurons is a slow process. Nonetheless, *Ikbkap*$^{flox/flox}$ mice still exhibit impaired temperature perception in adulthood.

Despite the clinical variability in autonomic impairment, FD patients already display autonomic dysfunction at birth or early infancy, such as poor suck at birth, inappropriate body temperature control and lack of emotional overflow tears, whereas older patients develop additional symptoms related to progressive dysautonomia, including cardiovascular and renal dysfunctions (3,7,37,38). Longitudinal studies involving re-testing of patients 13 years after the initial screening also support the notion that autonomic functions further deteriorate over time (47). Our analyses indicate that the development of SCG is significantly compromised in *Ikbkap*$^{\Delta 20/flox}$ mice and to a much lesser extent in *Ikbkap*$^{flox/flox}$ mice. However, extensive neurodegeneration occurs in *Ikbkap*$^{flox/flox}$ SCGs early after birth and progresses into adulthood (Fig. 4), suggesting that most of the SCG neuronal cell loss occurs postnatally in FD. These observations imply that therapies aiming at increasing full-length IKAP expression postnatally (52–57) might prevent further degeneration of sympathetic neurons in FD patients.

It is hypothesized that severe reduction in full-length IKAP expression is the leading or sole cause of FD, and that the truncated IKAP protein (derived from the Ikbkap mRNA that lacks exon 20) is either unstable or does not possess any deleterious gain-of-function (3,13,53,57). Strongly supporting this view is the fact that FD is a recessive disorder and carriers do not exhibit any signs of the disease (3,53). Based on these observations, it has been suggested that the extensive variability in the severity of the disease among FD patients, both within

and between families, might be a result of differences in expression levels of full-length IKAP protein (12). Although confirmation in FD patients awaits further investigation, our results strongly support this hypothesis. Even though our *Ikbkap*$^{\Delta 20/flox}$ mice do not carry the FD major haplotype, at the molecular level the consequence of the generated mutation is the same, that is, extremely reduced WT Ikbkap mRNA levels (from the flox allele) and expression of an Ikbkap mRNA lacking exon 20 (from the Δ20 allele). Similar to FD carriers, *Ikbkap*$^{\Delta 20/+}$ mice do not display any abnormalities, even at 24 months of age. In contrast, *Ikbkap*$^{flox/flox}$ mice do not express an mRNA lacking exon 20 but still develop FD features. These observations indicate that the expression of an mRNA lacking exon 20 (and consequently of a truncated IKAP protein) is not necessary to model FD. Notably though, FD phenotypic features are considerably milder in *Ikbkap*$^{flox/flox}$ mice compared with *Ikbkap*$^{\Delta 20/flox}$ mice (Fig. 2–4, and Table 2). Since both lines are maintained in the same genetic background, and the only biologically significant difference between them is the relative levels of IKAP expression (5% WT levels of full-length IKAP for *Ikbkap*$^{\Delta 20/flox}$ mice and 10% WT levels of full-length IKAP for *Ikbkap*$^{flox/flox}$ mice), our results strongly support the hypothesis that the extensive variability in FD clinical and pathological manifestations are likely due to slight differences in IKAP protein levels. The implications of these findings are significant not only in terms of the disease process, but also in what concerns possible therapeutic strategies, since our data indicate that treatments aiming at increasing IKAP expression might be successful even if they result in a small IKAP increase.

In conclusion, the availability of two mouse models that recapitulate FD phenotypic and neuropathological findings provide a means for further understanding the mechanisms underlying FD and for the development of potential new therapeutic interventions not only for FD, but also for other PNS disorders. In addition, of particular importance for therapeutic interventions is our finding that a slight increase in IKAP levels is sufficient to decrease disease severity and increase life span.

MATERIALS AND METHODS

Generation of mice carrying a conditional inactivation Ikbkap allele

The detailed descriptions of the original targeting vector to generate the targeted *Ikbkap3loxP* allele, as well as of the strategy to generate the *IkbkapΔ20* allele have been presented elsewhere (32). To generate mice carrying a conditional inactivation *Ikbkap* allele (*Ikbkap*$^{flox/+}$), we crossed the previously generated mouse line that carries a 3loxP-targeted Ikbkap allele (32) with a Cre transgenic line (HsCre6, maintained in the C57BL/6 background) that produces partial recombination events (33). Among the F1 mice that carried the targeted *Ikbkap* allele, mosaic mice that contained a mixture of recombination products between different pairs of loxP sites were selected and were then crossed with WT C57BL/6 mice. Analyses of the F2 progeny allowed for the identification of mice that had only the neo cassette excised and therefore contained a neoless (*Ikbkap*$^{flox/+}$) conditional allele (Dietrich *et al*., manuscript in preparation).

PCR assays for genotyping

For routine genotyping of progeny, genomic DNA was prepared from tail biopsies and PCR amplification reactions were carried out in the following conditions: 35 cycles consisting of 45 s denaturation at 94°C, 45 s annealing at 61°C and 1 min extension at 72°C as described previously (32) using the following primers:

Ikap-1 (forward): 5′-TGATTGACACAGACTCTGGCCA-3′;
Ikap-2 (reverse): 5′-GGAGATCCTCTAAGCAGCAGG-3′;
Ikap-3 (forward): 5′-CAGATTCGGAAGTGGCTGGAC-3′;
Ikap-4 (reverse): 5′-CTTTCACTCTGAAATTACAGGAAG-3′;
pgk (reverse): 5′-AGCGCATGCTCCAGACTGCC-3′.

Western blotting

Protein extracts from adult forebrain and E16.5 brains were obtained by homogenizing tissue in RIPA buffer (150 mM NaCl, 50 mM Tris (pH 8.0) 1% NP-40, 0.1% SDS, 0.5% sodium deoxycholate) containing protease inhibitor cocktail (Roche). Insoluble debris was discarded after centrifugation, and protein concentration was determined by the Bradford assay (Bio-Rad). Approximately 50 μg of protein was separated by SDS–PAGE (8% gel) and transferred into nitrocellulose membranes. Membranes were blocked in 5% non-fat milk for 1 h at room temperature and incubated overnight at 4°C with rabbit polyclonal antibody against the C-terminus region of IKAP (AnaSpec, 1:500), or mouse monoclonal antibody against β-tubulin (Chemicon, 1:5000). Membranes were washed and incubated with secondary antibodies for 1 h at room temperature. Protein bands were visualized by chemiluminescence (PIERCE or Amersham) followed by exposure to autoradiographic film.

Histological analyses

For histology, embryos and tissues were collected and fixed in 4% paraformaldehyde in phosphate-buffered saline (PBS) for at least 1 week; incubated for 24 h at 4°C in PBS containing 0.25 M sucrose and 0.2 M glycine; dehydrated; cleared with toluene and embedded in paraffin. Paraffin blocks were sectioned at 7 μm, mounted in superfrost slides (Fisher) and stained with hematoxylin and eosin (H&E).

Volumetric determination of sympathetic and sensory ganglia

Volumes of sympathetic and sensory ganglia were determined essentially as described (59). In brief, H&E-stained serial paraffin sections (7 μm) spanning the whole ganglia were analyzed under a Zeiss stereomicroscope, and the width and the length were measured every fifth section. Volumetric measurements were performed by calculating and adding the volumes between every section analyzed.

Neuronal counts in sympathetic ganglia

Neuronal counts were performed essentially as described (60). Briefly, E18.5 embryos and dissected ganglia were paraffin-embedded and sectioned at a thickness of 7 μm. Neurons with clearly visible nucleoli were counted from photomicrographs of H&E-stained paraffin sections. Total neuronal numbers were estimated based on the total volume of the ganglia.

Neuronal profiling of DRGs

For counts of DRG neurons, neurons with clearly visible nucleoli were counted from photomicrographs of H&E-stained paraffin sections. Sections were 7 μm thick, and neurons were counted in five sections per ganglion, at 50 μm intervals. Large light and small dark cells (45) were scored and counted in defined areas encompassing 40–50 neurons each.

Methylene blue staining of tongues

Fungi form papillae on the tongues were visualized by methylene blue staining, as described (61,62). In brief, tongues were dissected out in PBS and fixed in 4% PFA for 2 weeks. Tongues were then rinsed with PBS and stained by incubation in 0.5% methylene blue solution for 15–20 min at room temperature, followed by three brief washes in PBS. Fungiform papillae were counted on both sides of the median fissure in the anterior part of the tongue, as well as in middle and posterior regions of the tongue under a Zeiss stereomicroscope.

Immunohistochemistry

For immunohistochemistry on paraffin sections, slides were deparaffinized, rehydrated and incubated with 0.3% H_20_2 in methanol for 20 min, to quench endogenous peroxidase. Sections were then washed with PBS, blocked for 1 h with 4% BSA, 0.2% Triton X-100 in PBS and incubated at 4°C for 48–72 h with primary rabbit polyclonal antibody anti-TH (AB 152 Chemicon, 1: 200), or anti-CGRP (PC205L Calbiochem 1:200) in 0.4% BSA; 0.2% Triton X-100 in PBS. After several washes in PBS, primary antibody detection was carried out using the Vector ABC kit according to the manufacturer's instructions, followed by incubation with Fast DAB with metal enhancer (Sigma) or DAB brown substrate (BD Biosciences).

Temperature perception test

An incremental hot plate (IITC Model PE34 Hot/Cold Plate) was used to determine temperature perception thresholds. The conditions of the experiments were: stand-by temperature: 30°C, ramp: 5°C/min and cut-off temperature: 53°C. Experiments were performed on age-matched WT, *Ikbkap*$^{\Delta 20/flox}$ and *Ikbkap*$^{flox/flox}$ mice, and we used the first-evoked nocifensive behavior (hindpaw licking or jumping) as an end-point criterion. Mice were initially acclimated with the new environment for 30 min, submitted to the test and then allowed to rest for 1 h between each repetition. Three independent determinations were performed for each mouse.

SUPPLEMENTARY MATERIAL

Supplementary Material is available at *HMG* online.

ACKNOWLEDGEMENTS

We thank the Dysautonomia Foundation, Inc. for their interest in our research, and in particular David Brenner for discussions and support. We would also like to thank Adam and Justin Sachs for inspiration and encouragement.

Conflict of interest statement. None declared.

FUNDING

This work was supported by the National Institutes of Health (NS050376, NS061842 to I.D.).

REFERENCES

1. Riley, C.M., Day, R.L., Greely, D. and Langford, W.S. (1949) Central autonomic dysfunction with defective lacrimation; report of five cases. *Pediatrics*, **3**, 468–478.
2. Axelrod, F.B., Nachtigal, R. and Dancis, J. (1974) Familial dysautonomia: diagnosis, pathogenesis and management. *Adv. Pediatr.*, **21**, 75–96.
3. Axelrod, F.B. (2004) Familial dysautonomia. *Muscle Nerve*, **29**, 352–363.
4. Pearson, J. and Pytel, B.A. (1978) Quantitative studies of sympathetic ganglia and spinal cord intermedio-lateral gray columns in familial dysautonomia. *J. Neurol. Sci.*, **39**, 47–59.
5. Axelrod, F.B. and Pearson, J. (1984) Congenital sensory neuropathies. Diagnostic distinction from familial dysautonomia. *Am. J. Dis. Child*, **138**, 947–954.
6. Hilz, M.J., Axelrod, F.B., Bickel, A., Stemper, B., Brys, M., Wendelschafer-Crabb, G. and Kennedy, W.R. (2004) Assessing function and pathology in familial dysautonomia: assessment of temperature perception, sweating and cutaneous innervation. *Brain*, **127**, 2090–2098.
7. Goldstein, D.S., Eldadah, B., Sharabi, Y. and Axelrod, F.B. (2008) Cardiac sympathetic hypo-innervation in familial dysautonomia. *Clin. Auton. Res.*, **18**, 115–119.
8. Brunt, P.W. and McKusick, V.A. (1970) Familial dysautonomia. A report of genetic and clinical studies, with a review of the literature. *Medicine*, **49**, 343–374.
9. Mass, E., Wolff, A. and Gadoth, N. (1996) Increased major salivary gland secretion in familial dysautonomia. *Dev. Med. Child. Neurol.*, **38**, 133–138.
10. Gadoth, N., Mass, E., Gordon, C.R. and Steiner, J.E. (1997) Taste and smell in familial dysautonomia. *Dev. Med. Child Neurol.*, **39**, 393–397.
11. Anderson, S.L., Coli, R., Daly, I.W., Kichula, E.A., Rork, M.J., Volpi, S.A., Ekstein, J. and Rubin, B.Y. (2001) Familial dysautonomia is caused by mutations of the IKAP gene. *Am. J. Hum. Genet.*, **68**, 753–758.
12. Slaugenhaupt, S.A., Blumenfeld, A., Gill, S.P., Leyne, M., Mull, J., Cuajungco, M.P., Liebert, C.B., Chadwick, B., Idelson, M., Reznik, L. *et al.* (2001) Tissue-specific expression of a splicing mutation in the IKBKAP gene causes familial dysautonomia. *Am. J. Hum. Genet.*, **68**, 598–605.
13. Cuajungco, M.P., Leyne, M., Mull, J., Gill, S.P., Lu, W., Zagzag, D., Axelrod, F.B., Maayan, C., Gusella, J.F. and Slaugenhaupt, S.A. (2003) Tissue-specific reduction in splicing efficiency of IKBKAP due to the major mutation associated with familial dysautonomia. *Am. J. Hum. Genet.*, **72**, 749–758.
14. Axelrod, F.B., Iyer, K., Fish, I., Pearson, J., Sein, M.E. and Spielholz, N. (1981) Progressive sensory loss in familial dysautonomia. *Pediatrics*, **67**, 517–522.
15. Axelrod, F.B. (2005) Familial dysautonomia: a review of the current pharmacological treatments. *Expert Opin. Pharmacother.*, **6**, 561–567.
16. Cohen, L., Henzel, W.J. and Baeuerle, P.A. (1998) IKAP is a scaffold protein of the IkappaB kinase complex. *Nature*, **395**, 292–296.
17. Winkler, G.S., Petrakis, T.G., Ethelberg, S., Tokunaga, M., Erdjument-Bromage, H., Tempst, P. and Svejstrup, J.Q. (2001) RNA

polymerase II elongator holoenzyme is composed of two discrete subcomplexes. *J. Biol. Chem.*, **276**, 32743–32749.
18. Hawkes, N.A., Otero, G., Winkler, G.S., Marshall, N., Dahmus, M.E., Krappmann, D., Scheidereit, C., Thomas, C.L., Schiavo, G., Erdjument-Bromage, H. *et al.* (2002) Purification and characterization of the human elongator complex. *J. Biol. Chem.*, **277**, 3047–3052.
19. Close, P., Hawkes, N., Cornez, I., Creppe, C., Lambert, C.A., Rogister, B., Siebenlist, U., Merville, M.P., Slaugenhaupt, S.A., Bours, V., Svejstrup, J.Q. and Chariot, A. (2006) Transcriptional impairment and cell migration defects in elongator-depleted cells: implication for familial dysautonomia. *Mol. Cell*, **22**, 521–531.
20. Johansen, L.D., Naumanen, T., Knudsen, A., Westerlund, N., Gromova, I., Junttila, M., Nielsen, C., Bøttzauw, T., Tolkovsky, A., Westermarck, J. *et al.* (2008) IKAP localizes to membrane ruffles with filamin A and regulates actin cytoskeleton organization and cell migration. *J. Cell Sci.*, **121**, 854–864.
21. Cheishvili, D., Maayan, C., Cohen-Kupiec, R., Lefler, S., Weil, M., Ast, G. and Razin, A. (2011) IKAP/Elp1 involvment in cytoskeleton regulation and implication for familial dysautonomia. *Hum. Mol. Genet.*, **20**, 1585–1594.
22. Holmberg, C., Katz, S., Lerdrup, M., Herdegen, T., Jäättelä, M., Aronheim, A. and Kallunki, T. (2002) A novel specific role for I kappa B kinase complex-associated protein in cytosolic stress signaling. *J. Biol. Chem.*, **277**, 31918–31928.
23. Rahl, P.B., Chen, C.Z. and Collins, R.N. (2005) Elp1p, the yeast homolog of the FD disease syndrome protein, negatively regulates exocytosis independently of transcriptional elongation. *Mol. Cell*, **17**, 841–853.
24. Huang, B., Johansson, M.J. and Byström, A.S. (2005) An early step in wobble uridine tRNA modification requires the Elongator complex. *RNA*, **11**, 424–436.
25. Esberg, A., Huang, B., Johansson, M.J. and Byström, A.S. (2006) Elevated levels of two tRNA species bypass the requirement for elongator complex in transcription and exocytosis. *Mol Cell*, **24**, 139–148.
26. Lee, G., Papapetrou, E.P., Kim, H., Chambers, S.M., Tomishima, M.J., Fasano, C.A., Ganat, Y.M., Menon, J., Shimizu, F., Viale, A. *et al.* (2009) Modeling pathogenesis and treatment of familial dysautonomia using patient-specific iPSCs. *Nature*, **461**, 402–406.
27. Creppe, C., Malinouskaya, L., Volvert, M.L., Gillard, M., Close, P., Malaise, O., Laguesse, S., Cornez, I., Rahmouni, S., Ormenese, S. *et al.* (2009) Elongator controls the migration and differentiation of cortica neurons through acetylation of alpha-tubulin. *Cell*, **136**, 551–564.
28. Cornez, I., Creppe, C., Gillard, M., Hennuy, B., Chapelle, J.P., Dejardin, E., Merville, M.P., Close, P. and Chariot, A. (2008) Deregulated expression of pro-survival and pro-apoptotic p53-dependent genes upon Elongator deficiency in colon cancer cells. *Biochem. Pharmacol.*, **75**, 2122–2134.
29. Boone, N., Loriod, B., Bergon, A., Sbai, O., Formisano-Tréziny, C., Gabert, J., Khrestchatisky, M., Nguyen, C., Féron, F., Axelrod, F.B. and Ibrahim, E.C. (2010) Olfactory stem cells, a new cellular model for studying molecular mechanisms underlying familial dysautonomia. *PLoS One*, **5**, e15590.
30. Coli, R., Anderson, S.L., Volpi, S.A. and Rubin, B.Y. (2001) Genomic organization and chromosomal localization of the mouse IKBKAP gene. *Gene*, **279**, 81–89.
31. Cuajungco, M.P., Leyne, M., Mull, J., Gill, S.P., Gusella, J.F. and Slaugenhaupt, S.A. (2001) Cloning, characterization, and genomic structure of the mouse Ikbkap gene. *DNA Cell Biol.*, **20**, 579–586.
32. Dietrich, P., Yue, J., Shuyu, E. and Dragatsis, I. (2011) Deletion of exon 20 of the familial dysautonomia gene Ikbkap in mice causes developmental delay, cardiovascular defects, and early embryonic lethality. *PLoS One*, **6**, e27015.
33. Dietrich, P., Dragatsis, I., Xuan, S., Zeitlin, S. and Efstratiadis, A. (2000) Conditional mutagenesis in mice with heat shock promoter-driven cre transgenes. *Mamm. Genome*, **11**, 196–205.
34. Axelrod, F.B. and Dancis, J. (1973) Intrauterine growth retardation in familial dysautonomia. *Am. J. Dis. Child*, **125**, 379–380.
35. Smith, A., Farbman, A. and Dancis, I. (1965) Absence of taste-bud papillae in familial dysautonomia. *Science*, **147**, 1040–1041.
36. Kamboj, M.K., Axelrod, F.B., David, R., Geffner, M.E., Novogroder, M., Oberfield, S.E., Turco, J.H., Maayan, C. and Kohn, B. (2004) Growth hormone treatment in children with familial dysautonomia. *J. Pediatr.*, **144**, 63–67.
37. Rekhtman, Y., Bomback, A.S., Nash, M.A., Cohen, S.D., Matalon, A., Jan, D.M., Kaufmann, H., Axelrod, F.B., Radhakrishnan, J. and Appel, G.B. (2010) Renal transplantation in familial dysautonomia: report of two cases and review of the literature. *Clin. J. Am. Soc. Nephrol.*, **5**, 1676–1680.
38. Norcliffe-Kaufmann, L., Axelrod, F.B. and Kaufmann, H. (2011) Developmental abnormalities, blood pressure variability and renal disease in Riley Day syndrome. *J. Hum. Hypertens.*, 1 December. doi: 10.1038/jhh.2011.107.
39. Pearson, J., Pytel, B.A., Grover-Johnson, N., Axelrod, F. and Dancis, J. (1978) Quantitative studies of dorsal root ganglia and neuropathologic observations on spinal cords in familial dysautonomia. *J. Neurol. Sci.*, **35**, 77–92.
40. Lawson, S.N. and Waddell, P.J. (1991) Soma neurofilament immunoreactivity is related to cell size and fibre conduction velocity in rat primary sensory neurons. *J. Physiol.*, **435**, 41–63.
41. Tandrup, T. (1993) A method for unbiased and efficient estimation of number and mean volume of specified neurons subtypes in rat dorsal root ganglion. *J. Comp. Neurol.*, **329**, 269–276.
42. Gjerstad, M.D., Tandrup, T., Koltzenburg, M. and Jakobsen, J. (2002) Predominant neuronal B-cell loss in L5 DRG of p75 receptor-deficient mice. *J. Anat.*, **200**, 81–87.
43. Lawson, S.N. (1995) Neuropeptides in morphologically and functionally identified primary afferent neurons in dorsal root ganglia: substance P, CGRP and somatostatin. *Prog. Brain Res.*, **104**, 161–173.
44. Mu, X., Silos-Santiago, I., Carroll, S.L. and Snider, W.D. (1993) Neurotrophin receptor genes are expressed in distrinct patterns in developing dorsal root ganglia. *J. Neurosci.*, **13**, 4029–4041.
45. Tandrup, T. (1995) Are the neurons in the dorsal root ganglion pseudounipolar? A comparison of the number of neurons and number of myelinated and unmyelinated fibres in the dorsal root. *J. Comp. Neurol.*, **357**, 341–347.
46. Pearson, J., Brandeis, L. and Goldstein, M. (1979) Tyrosine hydroxylase immunoreactivity in familial dysautonomia. *Science*, **206**, 71–72.
47. Goldstein, D.S., Holmes, C. and Axelrod, F.B. (2008) Plasma catechols in familial dysautonomia: a long-term follow-up study. *Neurochem. Res.*, **33**, 1889–1893.
48. Diamond, G.A., D'Amico, R.A. and Axelrod, F.B. (1987) Optic nerve dysfunction in familial dysautonomia. *Am. J. Ophthalmol.*, **104**, 645–648.
49. Groom, M., Kay, M.D. and Corrent, G.F. (1997) Optic neuropathy in familial dysautonomia. *J. Neuroophthalmol.*, **17**, 101–102.
50. Mendoza-Santiesteban, C.E., Hedges, T.R. III, Norcliffe-Kaufmann, L., Warren, F., Reddy, S., Axelrod, F.B. and Kaufmann, H. (2012) Clinical neuro-ophthalmic findings in familial dysautonomia. *J. Neuroophthalmol.*, **32**, 23–26.
51. Macefield, V.G., Norcliffe-Kaufmann, L., Gutiérrez, J., Axelrod, F.B. and Kaufmann, H. (2011) Can loss of muscle spindle afferents explain the ataxic gait in Riley-Day syndrome? *Brain*, **134**, 3198–3208.
52. Hims, M.M., Ibrahim, E.C., Leyne, M., Mull, J., Liu, L., Lazaro, C., Shetty, R.S., Gill, S., Gusella, J.F., Reed, R. and Slaugenhaupt, S.A. (2007) Therapeutic potential and mechanism of kinetin as treatment for the human splicing disease familial dysautonomia. *J. Mol. Med. (Berl)*, **85**, 149–161.
53. Axelrod, F.B., Liebes, L., Gold-Von Simson, G., Mendoza, S., Mull, J., Leyne, M., Norcliffe-Kaufmann, L., Kaufmann, H. and Slaugenhaupt, S.A. (2011) Kinetin improves IKBKAP mRNA splicing in patients with familial dysautonomia. *Pediatr. Res.*, **70**, 480–483.
54. Anderson, S.L., Qiu, J. and Rubin, B.Y. (2003) Tocotrienols induce IKBKAP expression: a possible therapy for familial dysautonomia. *Biochem. Biophys. Res. Commun.*, **306**, 303–309.
55. Anderson, S.L. and Rubin, B.Y. (2005) Tocotrienols reverse IKAP and monoamine oxidase deficiencies in familial dysautonomia. *Biochem. Biophys. Res. Commun.*, **336**, 150–156.
56. Rubin, B.Y. and Anderson, S.L. (2008) The molecular basis of familial dysautonomia: overview, new discoveries and implications for directed therapies. *Neuromolecular Med.*, **10**, 148–156.
57. Keren, H., Donyo, M., Zeevi, D., Maayan, C., Pupko, T. and Ast, G. (2010) Phosphatidylserine increases IKBKAP levels in familial dysautonomia cells. *PLoS One*, **5**, e15884.
58. Hunnicutt, B.J., Chaverra, M., George, L. and Lefcort, F. (2012) IKAP/Elp1 is required *in vivo* for neurogenesis and neuronal survival, but not for neural crest migration. *PLoS One*, **7**, e32050.

59. Enomoto, H., Crawford, P.A., Gorodinsky, A., Heuckeroth, R.O., Johnson, E.M. Jr and Milbrandt, J. (2001) RET signaling is essential for migration, axonal growth and axon guidance of developing sympathetic neurons. *Development*, **128**, 3963–3974.
60. Ernfors, P., Lee, K.F., Kucera, J. and Jaenisch, R. (1994) Lack of neurotrophin-3 leads to deficiencies in the peripheral nervous system and loss of limb proprioceptive afferents. *Cell*, **77**, 503–512.
61. Sollars, S.I., Smith, P.C. and Hill, D.L. (2002) Time course of morphological alterations of fungiform papillae and taste buds following chorda tympani transection in neonatal rats. *J. Neurobiol.*, **51**, 223–236.
62. Ichikawa, H., Terayama, R., Yamaai, T., De Repentigny, Y., Kothary, R. and Sugimoto, T. (2007) Dystonin deficiency reduces taste buds and fungiform papillae in the anterior part of the tongue. *Brain Res.*, **1129**, 142–146.